Spiral fracture in metallic glasses and its correlation with failure criterion

Xianqi Lei [a], Yujie Wei [a,*], Bingchen Wei [a], Wei-Hua Wang [b]

[a] LNM, Institute of Mechanics, Chinese Academy of Sciences, Beijing 100190, PR China
[b] Institute of Physics, Chinese Academy of Sciences, Beijing 100080, PR China

A B S T R A C T

We report the observation of spiral fracture of the metallic glass $Zr_{41}Ti_{14}Cu_{12.5}Ni_{10}Be_{22.5}$ (at.%) subjected to both shear and normal stresses. The spiral angle (that between the spiral line and the loading axis) increases as we gradually change the normal stress from tensile (positive) to compressive (negative). The spiral nature of the fractured surface leads to a left-handed helix fractography pattern in tension, and a right-handed helix in compression. The Mohr–Coulomb type of failure is essential for the unique spiral fracture. The use of spiral angles resulted from torsion–tension experiments provide another novel experimental strategy to examine the failure criterion as well as stress state dependence of deformation mechanisms which lead to failure in metallic glasses.

© 2015 Acta Materialia Inc. Published by Elsevier Ltd. All rights reserved.

1. Introduction

The pressure sensitivity of failure in metallic glasses has been a topic of active research since the early experimental work of Davis and Kavesh [1] on ribbons, and more recent work by a number of authors [1–7]. This topic is tied to understanding the fundamental aspects of plastic deformation mechanisms which are still not fully understood [2,8]. Experimentally, the pressure sensitivity of failure can be directly examined by conducting experiments with superimposed hydrostatic pressure [1,3–7] in the manner of Bridgman [9], while any tension/compression asymmetry that exists at one atmosphere may also indicate some pressure sensitivity. For example, tension and compression tests conducted at one atmosphere by Donovan [10] found that the failure strength of $Pd_{40}Ni_{40}P_{20}$ followed the Mohr–Coulomb failure (M–C) criterion. Various works by Lewandowski et al. [3–7] found only a moderate normal stress or pressure sensitivity for tests conducted with superimposed hydrostatic pressure when analyzed with either a M–C or Drucker–Prager (D–P) criterion, despite relatively large changes in fracture angle [3–5] going from tension to compression at atmospheric pressure. This asymmetry in fracture angle was later shown to be influenced by stress concentrations at the sample/platen interface that biased the compression fracture angles, later rectified by the design of tapered grips [11,12]. Other recent work by Lu and Ravichandran [13] utilized confined compression

tests on $Zr_{41.2}Ti_{13.8}Cu_{12.5}Ni_{10}Be_{22.5}$ and found a more significant effect of confinement, although frictional restraint of the confining rings may have affected the magnitude of the pressure effect reported. Earlier work [14] utilized tension, compression, and torsion samples on a similar material and suggested that a von Mises criterion (i.e. pressure independent) might be appropriate. All of these previous works highlight the importance of continuing to examine the effects of changes in stress state and loading mode, as these have been observed to affect the deformation and fracture toughness, as shown by others [15–17].

In addition to experimental characterization, computational techniques were also employed to examine the validity of broadly used strength criteria including the Mohr–Coulomb criteria, Drucker–Prager criterion (D–P), and von Mises criterion. By using atomistic simulations, Lund and Schuh in 2004 [18] found that a pressure or normal stress dependence must be included in the failure criterion of metallic glasses, and they also suggested a range of Mohr–Coulomb internal friction coefficient of $\alpha = 0.12–0.4$ [19,20]. These atomistic simulations often produced much higher values for the friction coefficient than what was obtained experimentally, as well as what is found presently. Instrumented indentation and finite element simulations have also been employed to examine the pressure sensitivity of strength in BMGs [21–24] and they all suggested that pressure sensitive M–C or D–P [25] were better suited to capture deformation in structures with complex stress state. Finite-element modeling with embedded M–C criterion is able to captured typical features seen from systematic experimental characterizations of BMGs [26]. Later on simulations by Zhao and Li

* Corresponding author.
   E-mail address: yujie_wei@lnm.imech.ac.cn (Y. Wei).

[27] showed that taking consideration free volume dilatation [28] and the pressures sensitive D–P failure criterion are sufficient to explain the tension–compression fracture asymmetry in BMGs. Note that aforementioned experiments were typically performed at room temperature or temperature far below their respective glass transition temperatures of the tested materials. Recent work by Thamburaja et al. [29], guided by a series of molecular dynamics simulations conducted at low-homologous temperatures under homogeneous deformations, quantitatively prove that the continuum plastic behavior in metallic glasses could be described by the von Mises-type plastic yield criterion in that particular.

It is now generally accepted that criteria taking pressure sensitivity into account such as the M–C and the D–P are more appropriate to describe the strength of BMGs than pressure-independent ones like the Mises criterion when BMGs were tested at a temperature far below their glass transition temperature. However, regarding the exact formula to quantify the contribution of pressure to failure in BMGs, it remains an open question. For example, Zhang et al. suggested a modified M–C criterion where the internal friction parameters are different in tension and compression surface stress states [30]. Chen et al. [31] proposed an eccentric elliptical criterion on the basis of atomistic potential analysis. Later on, Wei [32,33] considered the different contributions of the distortional part and the volumetric part in total strain energy density to failure, and developed an energy based criterion where the shear strength and the normal strength are considered as two independent material parameters in BMGs. Recent experiments by Lei et al. [34] indeed found that distinct shear strength and normal strength are responsible for notch strengthening in BMGs: The tensile strength of the net section in circumferentially notched cylindrical BMGs increases with the constraint quantified by the ratio of notch depth over notch root radius. In summary, substantial understanding has been developed about the strength criterion of BMGs in the last two decades. Quantitatively, existing data about the material parameters of BMGs in different failure criteria are very scattered. There are compelling needs to critically examine the applicability of different failure criteria and to explore novel experimental strategies for calibration. In this work, we conducted combined torsion–tension experiments on $Zr_{41}Ti_{14}Cu_{12.5}Ni_{10}Be_{22.5}$ bulk metallic glass rods, and we further validated the applicability of Mohr–Coulomb failure criterion on the tested metallic glasses from the spiral fracture angle aspect. In contrast to the classic torsion–tension tests to a polycrystalline thin-walled tube by Taylor and Quinney in 1931

[35], the metallic glass could be better suited for failure analysis because the onset of plastic flow in polycrystalline materials is very likely to be influenced by preferred orientations of individual grains [36].

2. Experimental

We use probably the most well investigated BMG $Zr_{41}Ti_{14}Cu_{12.5}Ni_{10}Be_{22.5}$ (at.%). It represents a substantial amount of existing BMGs which offer almost no tensile ductility but exhibit intermediate-to-high resistance to fracture. The material is made in a water-cooled arc-melting hearth under a titanium-gathered argon atmosphere. Elemental metals (>99.9% purity) are used to form the master alloy and suction-casted into a $\varnothing$ 8 × 100 mm cylinders. Those cylinders are then lathed using carbide tool into dog-bone samples with dimensions shown as Fig. 1a and b. The gauged sections of the samples are then mirror-polished to smooth the surface. A servo-hydraulic MTS 809 test system is used to do the torsion–tension tests. We first exerted prescribed axial normal load within 20 s. This loading condition corresponds to a strain rate on the order of 10^{-3}/s since $Zr_{41}Ti_{14}Cu_{12.5}Ni_{10}Be_{22.5}$ breaks after an elastic strain limit about 0.02. We then twist the samples to failure. The torsion is applied at an angular velocity of 5°/min (corresponding to a maximum shear strain rate of about 2.5×10^{-4}/s). We also conducted contrast experiments with torsion loaded first (4 Nm/min, corresponding to a maximum shear strain rate about 1.2×10^{-5}/s), then axial load next (0.2 mm/min, corresponding to a strain rate about 2.5×10^{-4}/s), to character the normal–shear failure stresses combination's dependence on loading path. The range of the axial normal stress σ_0 (see Fig. 1c) for the tested samples is from $\sigma_0 = 1.98$ GPa (uniaxial tension) to $\sigma_0 = -1.84$ GPa, and is listed in detail in Table 1.

3. Results and discussion

As a BMG sample (see layout and dimensions in Fig. 1a and b) is subjected to mechanical twist while an exact axial load is applied, any material point in the sample is subjected to two stress components: the axial normal stress σ_0 and the shear stress (as illustrated in Fig. 1c). The shear deformation along the radial direction in a crossection perpendicular to the cylinder axis is linear in nature (as seen in Fig. 1d), resulting in a linear variation in shear stress
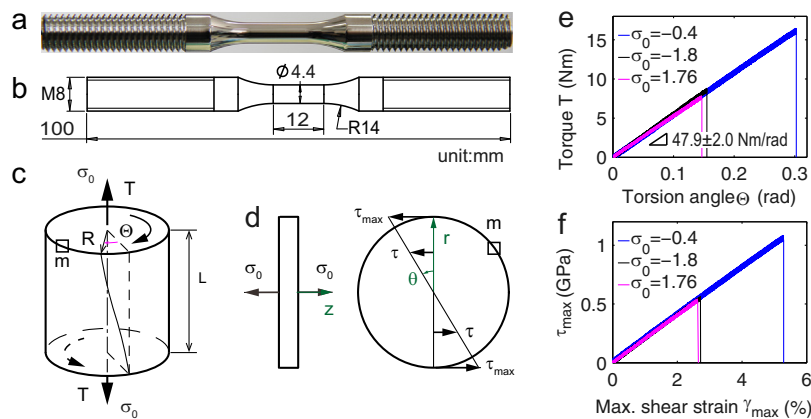
Fig. 1. Mechanical characterization of cylindrical metallic glass Zr_{41} $Ti_{14}Cu_{12.5}Ni_{10}Be_{22.5}$ subjected to both normal and shear stress. (a) Sample layout. (b) Dimensions of sample for normal loading-torsion tests (unit: mm). (c) Illustration of the loading: σ_0 – axial normal loading; T – torque; Θ – twisting angle; R – sample radius; L – length of interest; m – an arbitrary material point at the outermost surface. (d) Projected view to show normal stress σ_0 along the sample axis and radical shear stress τ distribution in the cross-section perpendicular to the normal direction; τ_{max} – the maximum shear stress at the outermost surface. (e) Typical torque versus twist angle curves at different axial normal stress; and we reach a stiffness of 47.9 ± 2.0 Nm/rad based on all experiments data listed in Table 1. (f) The maximum shear stress $\tau_{max}(\tau_{max} = 2T/\pi R^3)$ versus the maximum shear strain $\gamma_{max}(\gamma_{max} = \Theta R/L)$ at a material point in outermost surface.